Fabrication and AE Characteristics of TiNi/Al6061 Shape Memory Alloy Composite

Young-Chul Park*
Department of Mechanical Engineering, Donga University, Pusan 604-714, Korea
Jin-Kyung Lee
Department of Mechanical Engineering, Dongeui University, Pusan 614-714, Korea

TiNi/Al6061 shape memory alloy (SMA) composite was fabricated by hot press method to investigate the microstructure and mechanical properties. Interface bonding between TiNi reinforcement and Al matrix was observed by using SEM and EDS. Pre-strain was imposed to generate compressive residual stress inside composite. A tensile test for specimen, which underwent pre-strain, was performed at high temperature to evaluate the variation of strength and the effect of pre-strain. It was shown that interfacial reactions occurred at the bonding between matrix and fiber, creating two inter-metallic layers. And yield stress increased with the amount of pre-strain. Acoustic Emission technique was also used to nondestructively clarify the microscopic damage behavior at high temperature and the effect of pre-strain of TiNi/Al6061 SMA composite.

Key Words : Pre-Strain, Shape Memory Alloy (SMA), TiNi, Hot Press, Acoustic Emission

1. Introduction

Residual stress occurred when the difference of thermal expansion between fiber and matrix should be relieved to increase the strength of composite (Park et al., 2001 ; Oguocha et al., 2000 ; Kashiwagura et al. 2000). Moreover, inducing the compressive residual stress inside of composites could improve the tensile strength. TiNi alloy has been used to solve this residual stress since early 1980s (Garcia 2000 ; Ahrens 1999). TiNi (Shape Memory Alloy) has special quality of martensite transformation and superior function of shape recovery by this quality. After some forms of heat treatment, the TiNi alloy exists in the martensitic form at a room temperature. When the material is subject to plastic deformation, it undergoes a mechanical twinning process where each adjacent layer of atoms moves by one lattice parameter. However, when the material is heated, it undergoes a transformation phase to the austenite, the mechanical recovering imposed mostly deformation. In this study, smart composites with TiNi shape memory fiber (SMF) reinforcement was fabricated by hot press method and their mechanical properties were evaluated. The matrix is Al6061. The martensite transformation temperature depends on the chemical composition of alloy, method of fabrication and heat treatment. The objectives of this study are likely the next four sentences. First is studying the microstructures and mechanical properties were formed in the process of the fabrication of the TiNi/Al6061 shape memory alloy composites. Second is we identify the best processing condition of smart composites by hot pressing. Third is studying of tensile strength effects of the composites according to compressive residual stress by pre-strain. And finally, it is monitoring the failure mechanism and the damage behavior of composite corresponding to the variation of pre-strain by

* Corresponding Author,
E-mail : parkyc67@mail.donga.ac.kr
TEL : +82-51-200-7652; **FAX** : +82-51-200-7656
Department of Mechanical Engineering, Donga University, Pusan 604-714, Korea. (Manuscript **Received** August 12, 2003; **Revised** January 5, 2004)

using the acoustic emission (AE) technique (Liu et al., 2000 ; Emel'yanov et al., 2000 ; Enoki et al., 2001 ; Fregonese et al., 2001).

AE technique, which uses the elastic waves resulted from crack initiation and propagation in a material (Zyuryukin and Yu, 1999 ; Sukhodolsky et al., 1998 ; Smagin, 1999 ; Ahn and Nam, 2003), is a very useful method to evaluate fracture mechanism and microscopic damage of the composites.

2. Materials and Experimental Set-Up

2.1 Specimen fabrication

TiNi fiber (Ti-50.0 at.% Ni) of 500 μm diameter (made by Kantoc Ltd., Japan) and sheet metal of 6061 Al alloy were used to fabricate the smart composites. A hot press was designed for making aluminum alloy matrix composites reinforced by continuous TiNi shape memory alloy (SMA) fiber. The hot press of 250 ton with a hydraulic unit cylinder was used. A chamber was attached to the center of the hot press to keep the constant temperature. A fixture was designed for holding and arraying TiNi shape memory alloy strings as shown in Fig. 1. To investigate the effect of volume fraction and pre-strain, tensile test specimens (JIS 6) with several volume fractions were made by hot pressing method under the optimum processing condition (Yano et al., 1998 ; Shimoo et al., 1999). The TiNi fibers were fixed inside of 150 mm×22 mm 6061 Al sheets at constant spacing and these sheets were stuck between the press dies as shown in Fig. 2. TiNi/Al6061 composite was fabricated in the conditions of temperature of 833 K, pressure of 60 MPa, and 30 minutes in hot press. Moreover, because the surface of Al sheets can be oxidized easily in air, the hot press was preformed in Argon. A tensile test specimen of flat bar type was cut out from freeform as shown in Fig. 3. To determine the optimum conditions of the composites, the bonding state between 6061 Al matrix and TiNi fibers was observed by using the SEM images. Also, EPMA analysis was used to evaluate chemical compositions of the diffusion layer. Under the optimum conditions, TiNi/Al6061 composites with three different volume fractions of TiNi fibers (3.2, 5.2 and 7%)

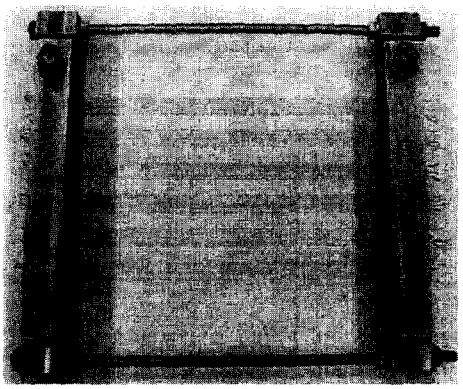

Fig. 1 The fixture for fixing and arraying SMA fibers

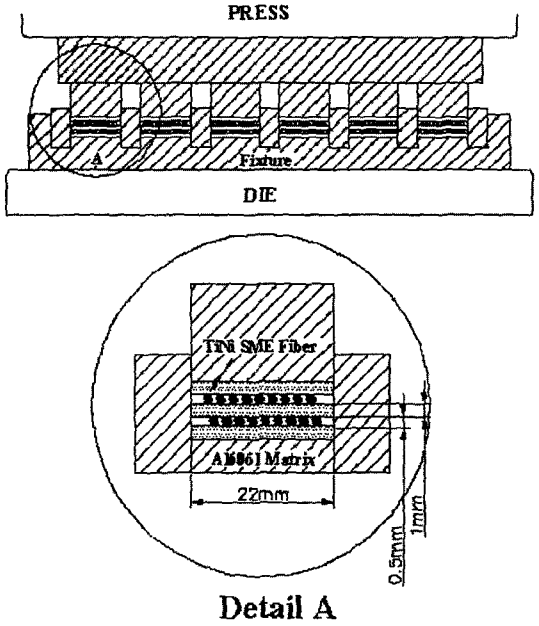

Fig. 2 Schematic diagram of hot pressing

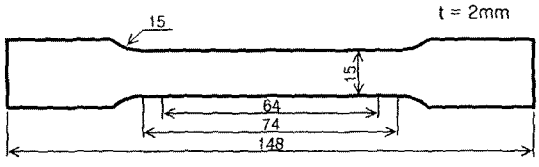

Fig. 3 The shape and dimensions of tensile test specimen (unit : mm)

were fabricated. T6 heat treatment was used to enhance the mechanical properties of the matrix. Solution treatments were conducted at 793 K and 813 K for 1 hour. As the final step of processing, the specimens were applied the kind of three type pre-strain (1, 3, and 5%) at room temperature. Mechanical testing was conducted on the pre-strained specimens at 363 K. Specimen temperature was measured on the surface of the specimen by using the thermocouples.

Figure 4 shows a cross-sectional view of the fabricated composites by the optimum processing condition. It shows that strong bonding was formed between the fiber and Al6061 matrix by the optimum processing condition and the bonded line on the each Al sheet disappeared. Figure 5 shows chemical composition changes through an interface between the matrix and the fiber by EPMA analysis. According to this result, thickness of the diffusion layer was about 4 μm.

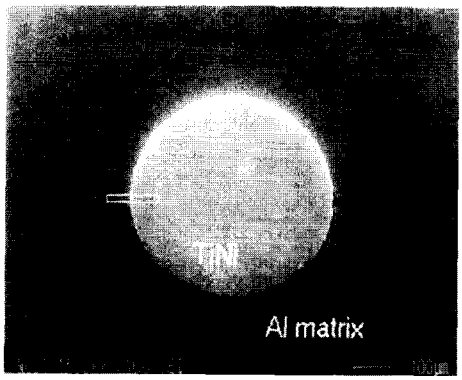

Fig. 4 SEM micrograph of the TiNi/Al6061 SMA composite

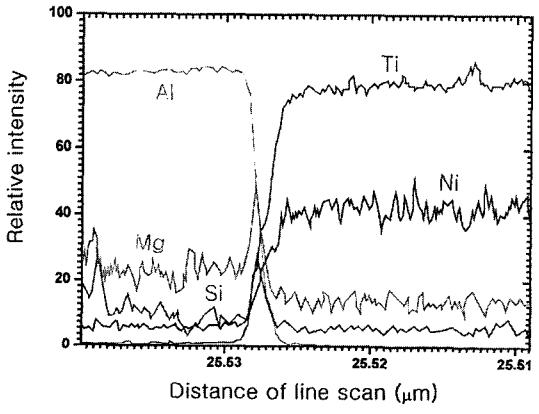

Fig. 5 EPMA analysis of the interface between fiber and matrix

2.2 Experimental apparatus

Tensile test was carried out to understand the microscopic fracture behavior and the degree of damage of TiNi/Al6061 composite by using the AE technique. The schematic diagram of the experimental set-up is illustrated in Fig. 6. The test was measured when a crosshead speed was 1.0 mm/min and an atmosphere temperature was 363 K. As the load increased, AE signals were generated by crack initiation and propagation within the specimen. These AE signals were detected by AE sensor (wide band) attached on the front surface of the specimen. The sensor output was amplified by 40 dB at the preamplifier and analyzed at the AE main board (MISTRAS 2001) by AE parameters (AE counts, duration time, amplitude, energy, etc.). The threshold level was fixed to 18.8 mV to eliminate electric and mechanical noises.

3. Results and Discussion

3.1 Stress-strain curves corresponding to pre-strain variation

In this study, in order to evaluate the effects of compressive residual stress between TiNi alloy and Al matrix at high temperature (363 K), 1, 3, and 5% pre-strains were applied to the TiNi/Al6061 composite. Figure 7 shows that tensile strength was the lowest in specimen, which did

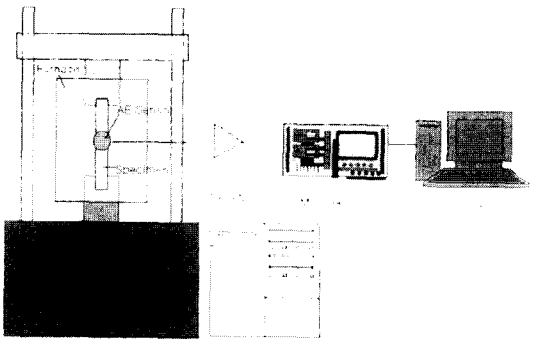

Fig. 6 Schematic diagram of experimental set-up

not undergo pre-strain. Tensile strength was gradually increased with pre-strain because of thermal elastic property of TiNi alloy. TiNi alloy shrank due to the phase transformation from martensite to austanite at 363 K, but Al matrix did not shrink at that temperature. Therefore, compressive residual stress was generated in composite by the difference of thermal expansion at the boundary between TiNi alloy and Al matrix. Also Tensile strength was increased with pre-strain due to the increase of compressive residual stress in TiNi/Al6061 composite.

3.2 Characteristics of AE signal corresponding to damage of TiNi/Al6061 composite

Figure 8 shows the characteristics of AE signals generated in the specimen with 3% pre-strain to clarify the microscopic damage behavior in TiNi/Al6061 composite. As shown in Fig. 8(a), it could be divided into four stages according to AE signal characteristics. Stage I, AE signals were not generated at the first stage of the load. Stage II, as the load increased gradually, about 5 AE signals were generated per second. Stage III, AE signals rapidly decreased at a point of 70% before the specimen was completely broken. Finally, AE signals increased at stage IV again. When the load was applied to the specimen, AE signals were not generated in the specimen because the specimen already underwent pre-strain. However, the load increased gradually and arrived at stage II, and then debonding at the boundary between TiNi alloy and Al matrix generated a lot of AE events. The debonding in composite decreased rapidly at the stage III and a few AE events happened in case of the plastic deformation of Al matrix, pulling out between TiNi alloy and Al matrix. This result implied that the debonding at the boundary between reinforcement and matrix was generated at the first stage of the load. When the load increased gradually, AE events decreased because the debonding was hardly generated and the composite was deformed rapidly. Only a few AE signals were generated by the plastic deformation of Al metrix and TiNi alloy at the threshold level of 45 dB through preliminary experience. Finally, when the load reached the stage IV, many AE events were generated by crack propagation into the TiNi/Al6061 composites and TiNi alloys fracture. However, energy of AE signals was distributed widely from 50 to 700. As shown in Fig 5(b), energy was distributed by 600 following to the form and magnitude of the debonding at stage II. AE signals under 50 in energy were observed at stage III due to plastic deformation of Al matrix, pulling out between TiNi alloy and Al matrix. A few AE signals above 600 in energy were observed as the large crack appeared and it was propagated into the composites. Finally TiNi alloy was broken at stage IV. Therefore, it was the microscopic damage behavior in TiNi/Al6061 composite by using the AE parameters such as

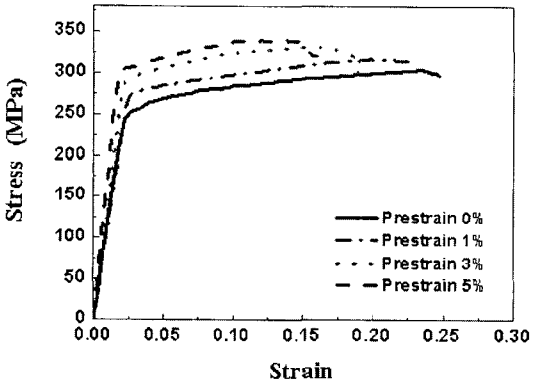

Fig. 7 Stress-strain curves of TiNi/Al6061 composites as a function of pre-strain at 363 K

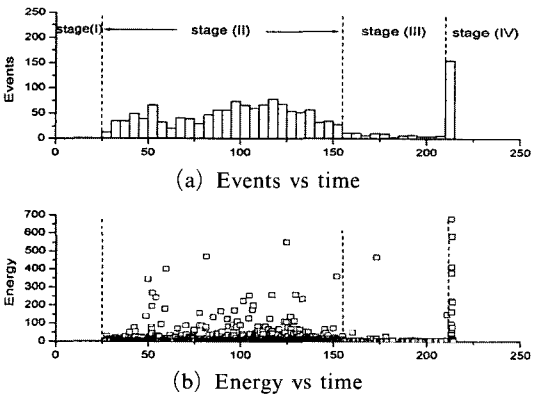

(a) Events vs time

(b) Energy vs time

Fig. 8 AE event, energy vs. time (sec) at 3% pre-strain composite (T=363K)

AE energy. And events could be evaluated.

3.3 AE signals characteristics corresponding to pre-strain variation

In order to evaluate the characteristics of pre-strain by using the AE technique, the characteristics of AE signals following to pre-strain variation were inspected. Figure 9 shows the relationship between cumulated AE counts and pre-strain variation. As shown in Fig. 9, a lot of AE counts were generated at the first stage of the load due to the boundary damage and stress concentration in the specimen that did not undergo pre-strain. The appearance of AE counts was generated alike at specimens of 1% and 3% pre-strain, but it generated lower counts in the 5% pre-strain. AE signal initiation in specimens of 1, 3, and 5% pre-strain was also delayed when we compared non pre-strained specimen.

Figure 10 shows the relationship between the AE events and pre-strain variation. A lot of AE events were generated by the boundary damage and stress concentration in non pre-strained specimen at the beginning of the load. However, the number of AE events decreased rapidly at a point of 70% of the complete fracture of the specimen. As shown in section 3.1, the reason was debonding phenomenon between reinforced TiNi alloy and Al matrix decreased rapidly, TiNi/Al6061 SMA composites was suddenly deformed with the load. When the composite was completely broken, many AE events were generated by the initiation and propagation of cracks, the fracture of TiNi alloys. The appearance of AE events was similar in three cases of 1, 3 and 5% pre-strain. However, when we compared the specimens of 1 and 3% pre-strain, AE events in the specimen of 5% pre-strain were the least generated. These results implied that AE events were hardly generated until at a point of 40% of the complete fracture of specimen by the offset of the internal compressive residual stress and external tensile stress. Tensile stress was generated in composite after 40% of the complete fracture and AE events were generated by the cause of boundary damage between Al6061 matrix and reinforced TiNi alloy.

From the results of AE events shown in Fig 10, when the stage of the sudden reduction appeared in the AE events, it means that the specimen is reached at a point of 70% of the complete fracture of composite.

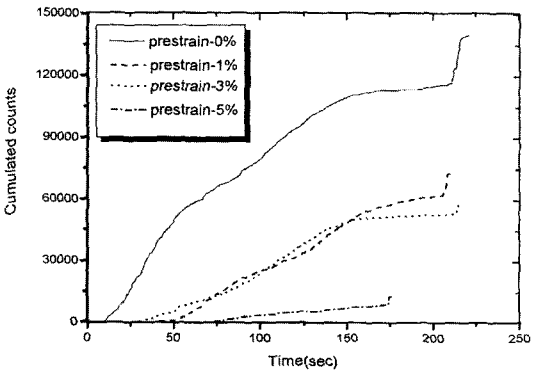

Fig. 9 AE counts vs. time according to pre-strain variation

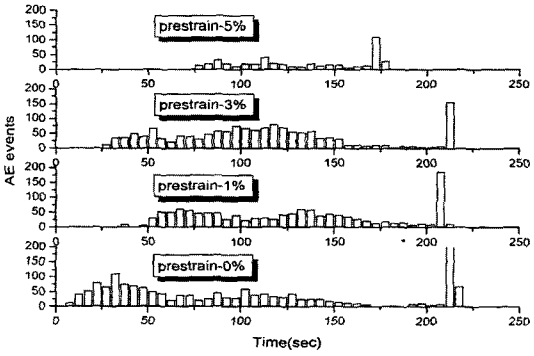

Fig. 10 AE events according to pre-strain variation

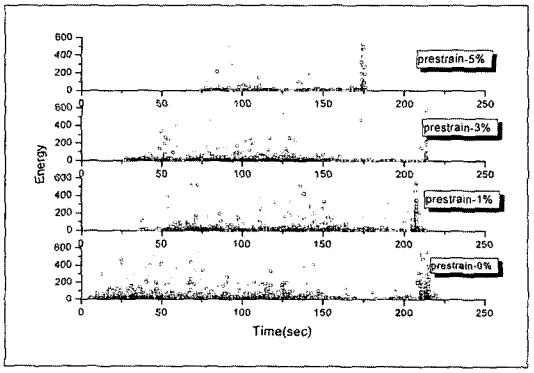

Fig. 11 AE energy according to pre-strain variation

Figure 11 shows the relationship between AE energy and pre-strain variation. As shown in Fig. 8, AE energy showed the range of distribution from 0 to 600 in all specimens with 1, 3, and 5% pre-strain. The energy range was widely distributed according to degree of damage at each stage including the boundary damage between the reinforced TiNi and Al6061 matrix. And the number of AE signal counts above 200 in energy decreased with pre-strain increase. AE signals under 100 in energy were observed from a point of 70% of complete fracture in all the specimen of 1% pre-strain. Then, pulling out and plastic deformation of TiNi/Al6061 SMA composite generated AE signals. But the cause was not by the boundary damage. However, the waveform and frequency spectrum of AE signals were inspected to clarify the microscopic damage mechanism of TiNi/Al6061 SMA composite under tensile loading.

4. Conclusions

From the application of AE technique to clarifying the fracture mechanism of TiNi/Al6061 SMA composite, the following conclusions were obtained.

(1) 1, 3, and 5% pre-strains were applied to the specimen to evaluate the effect of compressive residual stress at the boundary between Al matrix and TiNi reinforcement, and then tensile strength was increased by increase of pre-strain.

(2) From the results of the microscopic damage evaluation of TiNi/Al6061 SMA composite with applying the pre-strain by using the AE technique, it could be divided into four stages corresponding to the AE signals

i) Stage I — the load was increased but AE signals were not generated.

ii) Stage II — AE events were above 5 per second and AE signals above 600 in energy due to the boundary damage between the matrix and reinforcement.

iii) Stage III — A few AE events and AE signals under 50 in energy were by the plastic deformation of composite.

iv) Stage IV — A lot of AE events and AE signals above 700 in energy were by the fracture of TiNi alloy.

(3) In spite of the pre-strain increase, the generating appearance of AE signals and the energy range were not changed. However, the generating point of AE signal was delayed with the pre-strain increase.

References

Ahn, S. H. and Nam, K. W., 2003, "Characteristics of Elastic Waves Generated by Fatigue Crack Penetration and Growth in an Aluminum Plate," *KSME Journal*, Vol. 17, No. 11, pp. 1599~1607.

Ahrens, M., 1999, "Structural Integration of Shape Memory Alloys for Turbomachinery Applications," *Proceedings of SPIE Smart Structures and Materials 1999 Industrial and Commercial Applications of Smarts Structures Technologies*, pp. 426~435.

Emel'yanov, Yu. S., Batist, De., Golyandin, Kustov, S., Nikanorov, Pugachev, Sapozhnikov, G.K., Schaller, R., Sinani, A. and Van Humbeeck, J., 2000, "Detection of Shock-Wave-Induced Internal Stresses in Cu-Al-Ni Shape Memory Alloy by Means of Acoustic Technique," *Scripta Materialia 43 (12)*, pp. 1051~1057.

Enoki, M., Kishi, T. and Ohtake, S., 2001, "Classification of Micro-Fracture Process Type in Glass Matrix Composites by Quantitative Acoustic Emission Method," *Materials Transactions*, Vol. 42, No. 1, pp. 108~113.

Fregonese, M., Cetre, Y., Idrissi, H., Mazille, H. and Renaud, L., 2001, "Monitoring Pitting Corrosion of AISI 316L Austenitic Stainless Steel by Acoustic Emission Technique: Choice of Representative Acoustic Parameters," *J. of Materials Science*, Vol. 36, No. 3, pp. 557~563.

Garcia, J. R., 2000, "Stabilization of Martensite in Cu-Zn-Al Shape Memory Alloys: Effects of Precipitates and Thermal Cycling," *Scripta Materialia 42 (6)*, pp. 531~536.

Kashiwagura, N., Iwata, S., Jin, J. Y., Kamioka, H. and Ohsawa, Y., 2000, "Ultrasonic Behavior of Ti0.49-Ni0.51 Shape Memory Alloy Between 0℃ and 90℃," *Japanese Journal of Applied Physics*

Part 1-Regular Papers Short Notes & Review Papers, Vol. 39, No. 5B, pp. 2928~2932.

Liu, M., Liu, L., Li, Y. Y., Shelyakov, A. V. and Zhang, X. M., 2000, "In Situ TEM Observations of Martensite-Austenite Transformations in a Ni49Ti36Hf15 High Temperature Shape Memory Alloy," *J. of Materials Science Letters*, Vol. 19, No. 15, pp. 1383~1386.

Oguocha, INA., Radjabi, M. and Yannacopoulos, S., 2000, "The Effect of Cooling Rate on the Quench Sensitivity of 2618 Al/Al2O3 MMC," *J. of Materials Science*, Vol. 35, No. 22, pp. 5629~5634.

Park, B. G., Crosky, A. G. and Hellier, A. K., 2001, "Material characterization and Mechanical Properties of Al2O3-Al Metal Matrix Composites," *J. of Materials Science*, Vol. 36, No. 10, pp. 2417~2426.

Shimoo, T., Okamura, K., Seguchi, T. and Tsukada, I., 1999, "Thermal Stability of Low-SiC Fiber (Hi-Nicalon) Treated in a Hot Isostatic Press," *J. of Am Ceram Soc*, Vol. 82, No. 12, pp. 3508~3512.

Smagin, G., 1999, "Nonlinear Absorption of Longitudinal Elastic Waves in Dislocationless Crystals," *Proceedings of the 1999 IEEE Ultrasonic Symposium-Vol. 1*, pp. 553~556.

Sukhodolsky, T. and Sukhodolsky, P. A., 1998, "Coherent Neating of Vector Waves in Active Spectroscopy of Elastic Light Scattering," *Proceedings of SPIE ICONO'98-Laser Spectroscopy and Optical Diagnostics : Novel Trends and Applications in Laser Chemistry, Biophysics, and Biomedicine*, pp. 101~108.

Yano, T., Budiyanto, K., Iseki, T. and Yoshida, K., 1998, "Fabrication of Silicon Carbide Fiber-Reinforced Silicon Carbide Composite by Hot-Pressing," *Fusion Engineering & Design*, Vol. 41, pp. 157~163.

Zyuryukin, Yu. A., 1999, "Coupled-Wave Method in the Theory of Light Diffraction by Elastic Waves in Crystals," *Proceedings of SPIE Saratov Fall Meeting '99-Laser Physics and Spectroscopy*, pp. 162~173.